

September 2008

Multiple impact regimes in liquid environment dynamic atomic force microscopy

John Melcher

Purdue University, jmelcher@purdue.edu

Xin Xu

Purdue University, xu55@purdue.edu

Arvind Raman

Birck Nanotechnology Center, Purdue University, raman@purdue.edu

Follow this and additional works at: <http://docs.lib.purdue.edu/nanopub>

Melcher, John; Xu, Xin; and Raman, Arvind, "Multiple impact regimes in liquid environment dynamic atomic force microscopy" (2008). *Birck and NCN Publications*. Paper 125.
<http://docs.lib.purdue.edu/nanopub/125>

This document has been made available through Purdue e-Pubs, a service of the Purdue University Libraries. Please contact epubs@purdue.edu for additional information.

Multiple impact regimes in liquid environment dynamic atomic force microscopy

John Melcher, Xin Xu, and Arvind Raman^{a)}

School of Mechanical Engineering and Birck Nanotechnology Center, Purdue University, West Lafayette, Indiana 47907, USA

(Received 21 July 2008; accepted 7 August 2008; published online 4 September 2008)

A canonical assumption in dynamic atomic force microscopy is that the probe tip interacts with the sample once per oscillation cycle. We show this key ansatz breaks down for soft cantilevers in liquid environments. Such probes exhibit “drum roll” like dynamics with sequential bifurcations between oscillations with single, double, and triple impacts that can be clearly identified in the phase of the response. This important result is traced to a momentary excitation of the second flexural mode induced by tip-sample forces and low quality factors. Experiments performed on supported biological membranes in buffer solutions are used to demonstrate the findings. © 2008 American Institute of Physics. [DOI: 10.1063/1.2976438]

Dynamic atomic force microscopy (dAFM) has proven to be an invaluable tool for nanoscale metrology, however, the interrogation of many biological samples require the dAFM cantilever to operate in liquid environments where its dynamics become complicated. Several articles have focused on cantilever dynamics in liquids,^{1–6} however, these works have considered only a single-mode model for the cantilever dynamics. An important recent development⁷ was the finding that a two-mode model was necessary to simulate the dynamics of soft cantilevers in liquids, even if the second mode frequency is not an integer multiple of the fundamental.

In this article, we demonstrate several regimes where oscillations with multiple impacts occur for soft cantilevers (stiffness ≤ 1 N/m) operating in liquids, whereas in ambient and vacuum conditions only one attractive and one repulsive regime (with a single impact) are known.^{8–10} We show that the onsets of multiple tap, drum roll like oscillations may be clearly identified in the phase of the response. Multiple impact oscillations have several interesting ramifications for dAFM data interpretation in liquids which thus far implicitly assumes single impact oscillations.

To model the dynamics of the cantilever in a liquid environment, a two-mode model for a magnetically excited¹¹ cantilever interacting with a sample is chosen,⁷

$$\frac{\ddot{q}_i}{\omega_i^2} + \frac{\dot{q}_i}{\omega_i Q_i} + q_i = \frac{F_i}{k_i} \cos(\omega t) + \frac{F_{ts}(Z + q_1 + q_2)}{k_i}, \quad (1)$$

where subscripts $i=1$ and 2 denote to the first and second eigenmode respectively, q_i are coordinates for the tip deflection in the respective eigenmode and dots represent temporal derivatives. F_i , k_i , Q_i , ω_i and $(i=1,2)$ refer to the equivalent forcing amplitudes and stiffnesses,¹² quality factors, natural frequencies of the first two eigenmodes, respectively, ω is the excitation frequency and $T=2\pi/\omega$ is the oscillation period. Our interest in this article is for the case when the excitation frequency equals the natural frequency of the first eigenmode in liquid ($\omega=\omega_1$). Finally, F_{ts} is the nonlinear tip-sample interaction force through which the response of the first and second eigenmode become coupled. For conservative interactions, F_{ts} depends only on the tip-sample gap $d=Z+q_1$

+ q_2 , where Z is the separation between the base and the sample. In this work, we consider only the Hertz contact model:^{13,14} $F_{ts}(d)=(4E^*\sqrt{R/3})(-d)^{3/2}$ for $d<0$ and otherwise zero, where $E^*=[(1-\nu_s^2)/E_s+(1-\nu_t^2)/E_t]^{-1}$, and E_t , E_s , ν_t , ν_s are Young’s moduli and Poisson’s ratios of the sample and tip, respectively, and R is the radius of the tip.¹⁵

Our investigation of the multiple impact regimes begins with numerical simulations of Eq. (1) for two commercial cantilevers frequently used for imaging applications in liquids: an Olympus Biolever ($k_1=0.036$ N/m, $k_2=1.4$ N/m, $Q_1=1.2$, $Q_2=2$, $\omega_1=2\pi\times 9.3$ kHz, $\omega_2=2\pi\times 72$ kHz, $F_2/F_1=-0.554$, and $R=30$ nm) and a magnetically coated Agilent MAClever ($k_1=0.1$ N/m, $k_2=10$ N/m, $Q_1=1.6$, $Q_2=4.3$, $\omega_1=2\pi\times 3.5$ kHz, $\omega_2=2\pi\times 28$ kHz, $F_2/F_1=-1.54$, and $R=50$ nm).¹⁶ The ratio of k_2/k_1 is greatly affected by the nondimensional tip mass m_{tip}/m_c , where m_c is the mass of the cantilever: $k_2/k_1(m_{tip}/m_c=0)=39$ and $k_2/k_1(m_{tip}/m_c=0.1)=74$.¹² Tip masses between 10% and 20% of the cantilever mass are typical for many dAFM cantilevers, and in the case of the MAClever, $m_{tip}/m_c=0.16$ was chosen to match experimental data. The Biolever was chosen for its unique characteristic of essentially zero tip mass and the ratio $k_2/k_1=39$ was verified experimentally.¹⁷ Finally, in the standard photodiode setup in dAFM, the interpreted deflection becomes $u=q_1+\chi q_2$, where χ is a sensitivity ratio between the first and second eigenmode.⁷ Based on their respective tip mass, $\chi=3.47$ and $\chi=5.26$ are calculated for the Biolever and MAClever, respectively. Let A and Φ represent the first harmonic amplitude and phase respectively of u and A_0 represent the unconstrained amplitude ($F_{ts}=0$). In what follows, we will focus on simulating u and Φ versus A/A_0 because they afford a direct comparison with experimental observables.

A simulation ($A_0=10$ nm, $\omega=2\pi\times 9.3$ kHz) of the Biolever approaching a mica sample ($E_s=60$ GPa) predicted single and double impact regimes as the Z separation was gradually reduced to zero at a rate of 1 nm/s. Examples of two oscillation cycles in the single, double, and triple impact regimes are provided in Fig. 1 and correspond to amplitude ratios $A/A_0=0.95$, $A/A_0=0.90$, and $A/A_0=0.50$, respectively. Impacts are indicated by a nonzero tip-sample interaction force. This is a typical sequence of multiple impact oscillations observed for soft cantilevers in liquids. The two-mode

^{a)}Electronic mail: raman@purdue.edu.

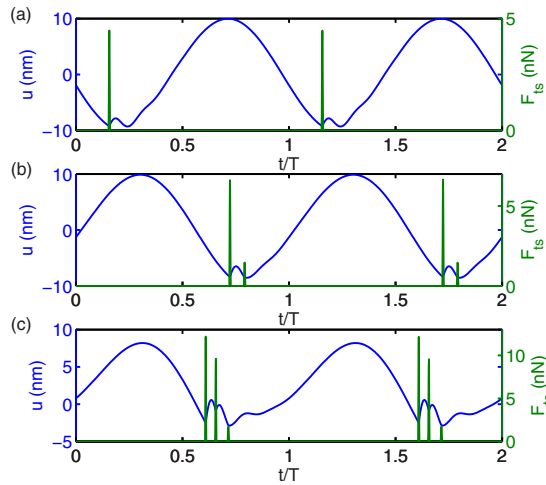


FIG. 1. (Color online) Numerical simulation of the photodiode deflection $u=q_1+\chi q_2$ for the Biolever in water tapping on mica. Examples of oscillations with (a) single, (b) double, and (c) triple impacts correspond to $A/A_0=0.95$, $A/A_0=0.90$, and $A/A_0=0.50$, respectively.

model is essential to accurately capture this physics; a point mass model would incorrectly predict these transitions at much lower amplitude ratios. The question now arises as to how multiple impact regimes may be identified in experiments where the tip-sample interaction force is not directly observed.

Many tip-sample interaction models applicable to dAFM, including the Hertz contact model used in these simulations, describe interaction forces that are nonsmooth functions of the tip-sample gap, where the nonsmoothness is localized at the point of contact between the tip and the sample.¹³ For these models, the possibility of a grazing bifurcation^{18,19} arises as some parameter, such as Z , is varied. At the boundary of each impact regime, there must exist a grazing trajectory where at least one impact occurs at zero velocity and a grazing bifurcation occurs. At this point, the current amplitude branch loses stability and a new stable branch is formed. Therefore, we expect that grazing trajectories, which indicate the onset of an impact regime, to be accompanied by abrupt behavior in the phase versus amplitude ratio curve (i.e., either a nonsmooth point or a discontinuous jump) resulting from a grazing bifurcation. If the sample is sufficiently soft, the idealization of a grazing bifurcation becomes strained, and we must rely on simulations for some indication of a grazing trajectory.

Numerical simulations of Eq. (1) for the Biolever [Fig. 2(a)] and the MAClever [Fig. 2(b)] approaching both a soft sample ($E_s=1$ GPa) and a stiff sample ($E_s=60$ GPa, mica) were performed. The phase Φ is plotted as a function of the amplitude ratio A/A_0 . Points in the phase corresponding to grazing trajectories with two (G2) and three (G3) impacts and mark the onsets of the double and triple impact regimes, respectively. Both nonsmooth points and discontinuous jumps are observed for the stiff sample. For the soft sample, the indication of a grazing trajectory is more subtle, however, a relatively abrupt transition in the phase still occurs.

Experimental measurements were made using an Agilent 5500 AFM system and the MAClever in salt buffer (300 mM KCl, 20 mM Tris-HCl). A sample consisting of patches of wild type purple membrane (PM) was diluted to approximately 0.05 mg/mL and deposited on freshly cleaved mica

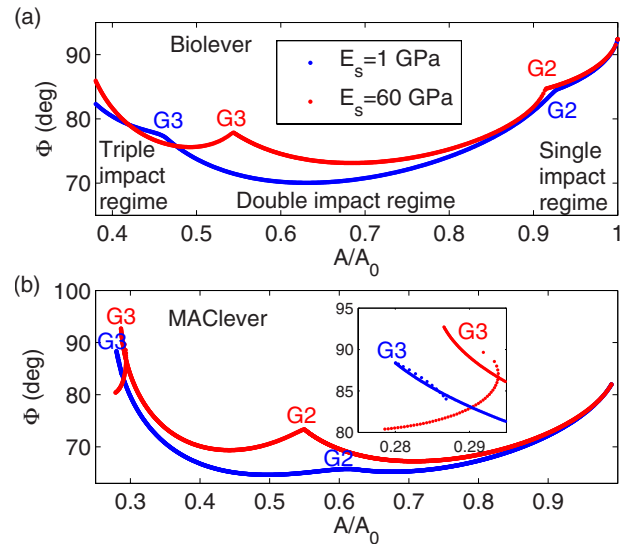


FIG. 2. (Color online) Numerical simulations of phase versus amplitude ratio for the (a) Biolever and (b) MAClever approaching a stiff sample (mica, $E_s=60$ GPa) and a soft sample ($E_s=1$ GPa). Grazing trajectories with two (G2) and three (G3) impacts mark the onset of the corresponding multiple impact regime.

in the buffer solution. In these experiments, first the sample is imaged in tapping mode ($A_0=20$ nm, $\omega=2\pi\times 3.3$ kHz) and secondly A and Φ are measured on locations corresponding to mica and a single layer of PM and converted to Φ versus A/A_0 , as shown in Fig. 3. Nonsmooth points in the phase indicated in Fig. 3 are expected to be the onsets of the double and triple impact regimes. Experiments on mica correspond excellently with simulations in Fig. 2(b) for the MAClever. However some differences are present in the measured phase response on PM (Fig. 3) and the theoretical prediction (Fig. 2) for the soft material. This is attributed to the fact that the soft ($E_s=50$ MPa), thin (6 nm) membrane rests on a stiff mica substrate and the mechanics of this system are not suitably captured with simple Hertz contact Nevertheless the transition from the single to double tap regime

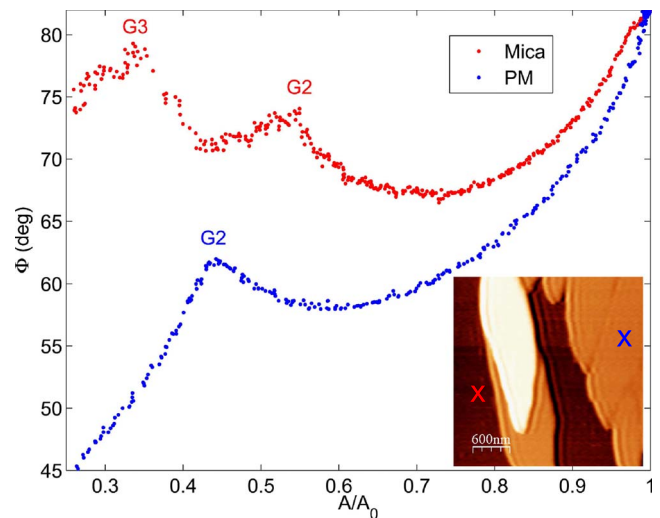


FIG. 3. (Color online) Experimental phase vs amplitude ratio on mica and a single layer of PM using the MAClever ($A_0=20$ nm, $\omega=2\pi\times 3.3$ kHz) in buffer solution. Nonsmooth points in the phase are attributed to grazing trajectories which mark the onset of the indicated multiple impact regime. Shown in the inset (Ref. 20) is the topography of PM deposited on mica and the approximate locations where the phase curves were extracted.

(G2) is clearly visible in the experimental phase data on PM in Fig. 3. Thus the onset oscillations with different numbers of taps per cycle can be unequivocally identified by the abrupt changes in the phase versus amplitude ratio plots.

In order to understand the factors upon which multiple impact regimes depend, it is useful to develop an approximate theory for the solution of Eq. (1) using an appropriate nonlinear perturbation method. Let us consider Eq. (1) ($i=1$) and apply a single term harmonic balance $q_1 = a \cos(\omega_1 t - \phi) = a \cos \theta$, where a and ϕ are the amplitude and phase, and we have limited the excitation frequency to $\omega = \omega_1$.²⁰ When approaching the sample from far away, the cantilever first grazes the surface and single impact oscillations occur. Substituting $q_1 = a \cos \theta$ into Eq. (1) ($i=1$), and collecting the $\cos \theta$ terms yields

$$F_1 \cos \phi + \frac{1}{\pi} \int_0^{2\pi} F_{\text{ts}}(Z + a \cos \theta + q_2) \cos \theta d\theta = 0. \quad (2)$$

F_1 can be eliminated from Eq. (2) by noting $F_1 = k_1 a_0 / Q_1$, where a_0 is the unconstrained amplitude of q_1 when $\omega = \omega_1$. Now we consider contact times $t_c \leq 0.2T$ in the neighborhood of $\theta = \pi$. Expanding $\cos \theta = -1 + O(\bar{\theta}^2)$, where $\bar{\theta} = \pi - \theta$ and substituting $d\theta = \omega_1 dt$, Eq. (2) can be used to approximate the tip-sample impulse \hat{F}_{ts} ,

$$\hat{F}_{\text{ts}} = \frac{\pi k_1 a_0}{Q_1 \omega_1} \cos \phi. \quad (3)$$

From Eq. (3) it becomes possible to estimate the dynamics of the second eigenmode which is governed by Eq. (1) ($i=2$). We can neglect the unconstrained response of q_2 (i.e., set $F_2=0$) since the excitation is well below the second resonance and $k_2 \gg k_1$. For stiff samples ($E_s \geq 5$ GPa), the contact time can be further restricted to $t_c \leq 0.2T_{2d}$, where $T_{2d} = 2\pi / \omega_{2d}$ and $\omega_{2d} = \omega_2 \sqrt{1 - 1/4Q_2^2}$. In this case, there is a momentary excitation of q_2 that may be approximated as an impulse response for single impact oscillations,

$$q_2(\bar{t}) = \left(\frac{a_0 \pi \omega_2^2 k_1}{Q_1 \omega_1 \omega_{2d} k_2} \cos \phi \right) e^{-\bar{t}/\tau} \sin(\omega_{2d} \bar{t}), \quad (4)$$

where $0 \leq \bar{t} < T$ has been translated to the moment of impact and $\tau = 2Q_2 / \omega_2$. For $Q_2 < \omega_2 / \omega_1$, q_2 will have decayed by more than 95% in amplitude by the time the tip approaches the sample again in the next oscillation. This condition is typically met for soft cantilevers in liquids. Thus the theory indicates that, in the single impact regime, the second eigenmode undergoes an impulse response at each impact and rings down before the next impact.

While Eq. (4) is restricted to stiff samples (small contact time) and relatively high amplitude ratios (single harmonic approximation of q_1), it reveals an essential difference between liquid and ambient/vacuum environment dAFM with regard to the source of momentary excitation. While ratios such as ω_2 / ω_1 or k_2 / k_1 change slightly when a soft cantilever is taken from ambient to a liquid environment, the quality factors drop by one to two orders of magnitude. A substantial decrease in Q_1 increases the tip-sample impulse [Eq. (3)] and results in a large momentary excitation [Eq. (4)]. The contribution of q_2 to the total tip-sample gap $d = Z + q_1 + q_2$ introduces the possibility of a double impact oscillation during the ring-down of q_2 . Further approaching the sample, higher

order impact oscillations (three, four, impacts per cycle) may occur, although the nature of these oscillations is generally more complex.

From the approximate analysis and numerical simulations of Eq. (1), nondimensional numbers that are important to multiple impacts can be determined. These parameters are $\lambda_1 = \omega_2^2 k_1 / \omega_1 \omega_{2d} k_2 Q_1$, which decides the initial amplitude of the momentary excitation of the second eigenmode, $\lambda_2 = \omega_{2d} / \omega_1$, which allows q_2 to ring while the tip is still in the proximity of contact and $\lambda_3 = Q_2 \omega_1 / \omega_2$, which determines the decay rate of the momentary excitation relative to the overall oscillation period T . As can be seen with the Biolever and the MAClever, these nondimensional parameters can vary substantially from one cantilever to another (for example, $\lambda_1^{\text{Bio}} / \lambda_1^{\text{MAC}} = 3.4$), which greatly influences the amplitude ratios where multiple impact regimes occur (Fig. 2).

To conclude, we have demonstrated multiple impact oscillations for soft cantilevers in liquid environments and shown how the boundaries between impact regimes can be identified by the phase of the response. Multiple impact regimes are one example of the crucial role of the momentary excitation of the second eigenmode for soft cantilevers in liquid environments. We expect many implications resulting from these drum roll like interactions between the tip the sample, particularly regarding imaging forces and compositional contrast. Characteristics of the tip-sample interaction, such as average and peak interaction forces, as well as quantities related compositional contrast, such as phase and higher harmonic content, are affected by multiple impacts.

This research was supported by the National Science Foundation under Grant No. CMMI-0700289. The authors thank Professor Ron Reifengerger (Physics, Purdue) for providing the bacteriorhodopsin and discussions.

¹C. A. J. Putman, K. O. Vanderwerf, B. G. Degrooth, N. F. Vanhulst, and J. Greve, *Appl. Phys. Lett.* **64**, 2454 (1994).

²P. K. Hansma, J. P. Cleveland, M. Radmacher, D. A. Walters, P. E. Hillner, M. Bezanilla, M. Fritz, D. Vie, H. G. Hansma, C. B. Prater, J. Massie, L. Fukunaga, J. Gurely, and V. Elings, *Appl. Phys. Lett.* **64**, 1738 (1994).

³G. Y. Chen, R. J. Warmack, P. J. Oden, and T. Thundat, *J. Vac. Sci. Technol. B* **14**, 1313 (1996).

⁴N. A. Burnham, O. P. Behrend, F. Oulevey, G. Gremaud, P. J. Gallo, D. Gourdon, E. Dupas, A. J. Kulik, H. M. Pollock, and G. A. D. Briggs, *Nanotechnology* **8**, 67 (1997).

⁵S. J. T. van Noort, O. H. Willemsen, K. O. van der Werf, B. G. de Grooth, and J. Greve, *Langmuir* **15**, 7101 (1999).

⁶J. Preiner, J. Tang, V. Pastushenko, and P. Hinterdorfer, *Phys. Rev. Lett.* **99**, 046102 (2007).

⁷S. Basak and A. Raman, *Appl. Phys. Lett.* **91**, 064107 (2007).

⁸B. Anczykowski, D. Kruger, and H. Fuchs, *Phys. Rev. B* **53**, 15485 (1996).

⁹L. Wang, *Appl. Phys. Lett.* **73**, 3781 (1998).

¹⁰R. Garcia and A. San Paulo, *Phys. Rev. B* **60**, 4961 (1999).

¹¹W. H. Han, S. M. Lindsay, and T. W. Jing, *Appl. Phys. Lett.* **69**, 4111 (1996).

¹²J. Melcher, S. Hu, and A. Raman, *Appl. Phys. Lett.* **91**, 053101 (2007).

¹³B. Cappella and G. Dietler, *Surf. Sci. Rep.* **34**, 1 (1999).

¹⁴H. Hertz and J. Reine, *J. Reine Angew. Math.* **92**, 156 (1881).

¹⁵The tip has elastic modulus of 130 GPa. All Poisson's ratios are 0.3.

¹⁶Parameters k_1 , ω_1 , ω_2 , Q_1 , and Q_2 are measured experimentally from the method of Sader in air and thermal spectra in water respectively. Ratios k_2/k_1 and F_2/F_1 are calculated theoretically for the assumed tip mass.

¹⁷J. E. Sader, I. Larson, P. Mulvaney, and L. R. White, *Rev. Sci. Instrum.* **66**, 3789 (1995).

¹⁸A. B. Nordmark, *J. Sound Vib.* **145**, 279 (1991).

¹⁹H. Dankowicz, X. P. Zhao, and S. Misra, *Int. J. Non-Linear Mech.* **42**, 697 (2007).

²⁰I. Horcas, R. Fernandez, J. M. Gomez-Rodriguez, J. Colchero, J. Gomez-Herrero, and A. M. Baro, *Rev. Sci. Instrum.* **78**, 013705 (2007).